THE FASEB JOURNAL • RESEARCH • www.fasebj.org

Sacsin, mutated in the ataxia ARSACS, regulates intermediate filament assembly and dynamics

Benoit J. Gentil,[*,†,1] Gia-Thanh Lai,[*,†] Marie Menade,[‡] Roxanne Larivière,[§] Sandra Minotti,[*] Kalle Gehring,[‡] J.-Paul Chapple,[¶] Bernard Brais,[§] and Heather D. Durham[*]

[*]Department of Neurology and Neurosurgery, Montreal Neurological Institute, [†]Department of Kinesiology and Physical Education, [‡]Department of Biochemistry, Groupe de Recherche axé sur la Structure des Protéines, and [§]Laboratory of Neurogenetics of Motion, Montreal Neurological Institute, McGill University, Montreal, Québec, Canada; and [¶]William Harvey Research Institute, Barts and the London School of Medicine and Dentistry, Queen Mary University of London, London, United Kingdom

ABSTRACT: Loss of sacsin, a large 520 kDa multidomain protein, causes autosomal recessive spastic ataxia of the Charlevoix-Saguenay, one of the most common childhood-onset recessive ataxias. A prominent feature is abnormal bundling of neurofilaments in many neuronal populations. This study shows the direct involvement of sacsin domains in regulating intermediate filament assembly and dynamics and identifies important domains for alleviating neurofilament bundles in neurons lacking sacsin. Peptides encoding sacsin internal repeat (SIRPT) 1, J-domains, and ubiquitin-like domain modified neurofilament assembly *in vivo*. The domains with chaperone homology, the SIRPT and the J-domain, had opposite effects, promoting and preventing filament assembly, respectively. In cultured *Sacs*$^{-/-}$ motor neurons, both the SIRPT1 and J-domain resolved preexisting neurofilament bundles. Increasing expression of heat shock proteins also resolved neurofilament bundles, indicating that this endogenous chaperone system can compensate to some extent for sacsin deficiency.—Gentil, B. J., Lai, G.-T., Menade, M., Larivière, R., Minotti, S., Gehring, K., Chapple, J.-P., Brais, B., Durham, H. D. Sacsin, mutated in the ataxia ARSACS, regulates intermediate filament assembly and dynamics. FASEB J. 33, 000–000 (2019). www.fasebj.org

KEY WORDS: chaperone proteins · rare neurological diseases · cytoskeleton

Autosomal recessive spastic ataxia of the Charlevoix-Saguenay (ARSACS) is a childhood-onset neurologic disorder caused by loss-of-function mutations in the *SACS* gene that encodes sacsin (*SACS*). ARSACS is the second most common cause of recessive ataxia, with >200 mutations described worldwide (1–5). Patients usually present with the classic triad of cerebellar ataxia, pyramidal spasticity, and motor sensory neuropathy with variable intellectual dysfunction and retinal changes (2, 6). *Sacs* knockout mice develop early ataxia, and as in human brains, abnormal bundling of neurofilaments (NFs) occurs in multiple neuronal populations, including Purkinje and cortical motor neurons (7). Peripheral neuropathy is also associated with ARSACS, and similar NF bundles were found in cultured *Sacs*$^{-/-}$ spinal motor neurons and dorsal root ganglion (DRG) sensory neurons. NF bundling occurred before impaired mitochondrial elongation and transport, another feature of ARSACS cells. Strikingly, bundling and collapse of the vimentin intermediate filament (IF) network and mitochondrial abnormalities also occur in ARSACS human fibroblasts in culture (8, 9), suggesting a role of sacsin in IF assembly and/or maintenance in multiple cell types.

The assembly of IFs is a complex and ordered process (10), and identifying how the loss of sacsin interferes with this process will shed light on the cellular pathophysiology of ARSACS. IF proteins form coiled-coiled dimers through association of their rod domains, and these dimers then further dimerize to form nonpolar tetramers through antiparallel association. Eight tetramers then associate laterally into nonionic detergent-insoluble precursors (*i.e.*, unit length filaments), which then anneal end-to-end into an immature filament of 18 nm. Radial compaction of the immature filament into a 10-nm mature filament is the final step of IF assembly (11). Once the filamentous structure has been formed, turnover can occur by severing and reannealing of the existing filament and by exchange of

ABBREVIATIONS: ARSACS, autosomal recessive spastic ataxia of the Charlevoix-Saguenay; DRG, dorsal root ganglion; FRAP, fluorescence recovery after photobleaching; gRNA, guide RNA; HEPN, higher eukaryotes and prokaryotes nucleotide-binding; HSD, honestly significant difference; HSP, heat shock protein; IF, intermediate filament; NF, neurofilament; NFH, neurofilament heavy polypeptide; NFL, neurofilament light polypeptide; NFM, neurofilament medium polypeptide; SacsJ, sacsin J-domain; SIRPT, sacsin internal repeat; TBS, Tris-buffered saline; UBL, ubiquitin-like domain

[1] Correspondence: Currie Gym Office A210, 475 Pine Ave. West, Montreal, QC, Canada H2W 1S4. E-mail: benoit.gentil@mcgill.ca

doi: 10.1096/fj.201801556R
This article includes supplemental data. Please visit *http://www.fasebj.org* to obtain this information.

individual subunits. However, the processes regulating the assembly and maintenance of the IF network are not well understood (10).

In mature neurons, the major IF proteins are the NF proteins neurofilament light polypeptide (NFL), neurofilament medium polypeptide (NFM), neurofilament heavy polypeptide (NFH), and peripherin (12). NFs are formed from assembly of a core protein (NFL, peripherin) with NFM and NFH to form a rod-like structure from which C-termini protrude (13). The C-termini of NFM and NFH protrude from the filament core and form cross-bridges to other NF, microtubules, and organelles. IF-associated proteins, such as plectins, also link cytoskeletal components with each other and with organelles to form the integrated, functional cytoskeleton (14).

Although IF proteins can assemble passively *in vitro*, we speculate that assembly and turnover *in vivo* would be highly regulated given the ordered complexity and dynamics of cytoskeletal networks and the inherent insolubility of IF proteins (15, 16). Assembly of NF and other IF proteins is inhibited by phosphorylation of head domain residues by second messenger–dependent protein kinases (17). In addition to regulation by phosphorylation, ordered NF assembly and turnover would involve other proteins that serve as chaperones important for filament maturation, regulating interactions and targeting for degradation. Key mechanisms that, when perturbed, could alter assembly of NFs in diseases include aberrant stoichiometry of NF subunits (18–22), NF phosphorylation (13, 23–25), disruption of NF chaperoning, and mutations in genes encoding NF proteins (26, 27).

Little is known about the chaperones that play a role in normal NF assembly and turnover. The small heat shock proteins (HSPs) HSPB1 (HSP25/27) and HSPB8 (HSP22) increase solubility of NF precursors (28), and mutations in their genes cause peripheral neuropathies with NF aggregates (Charcot-Marie-Tooth disease type 2 and distal hereditary motor neuropathy) (29, 30). Coexpression of the chaperone HSPA1A (HSP70-1) with aggregation-prone NFL mutants in motor neurons and in the adenocarcinoma cell line SW13^{vim-} lacking IFs prevented aberrant aggregation of mutant NF proteins and promoted their proper assembly into filamentous structures (31).

Sacsin is a gigantic protein comprising 4579 aa. According to *in silico* analysis, the protein includes several functional domains: an N-terminal ubiquitin-like (UBL) domain, 3 chaperone domains homologous to HSP90 in repeated specific internal regions [sacsin internal repeat (SIRPT)] (32–35) and a sacsin J-domain (SacsJ) followed by a C-terminal higher eukaryotes and prokaryotes nucleotide-binding (HEPN) domain (33, 36, 37). The presence in sacsin of chaperone and UBL domains, coupled with the observed bundling of IFs in many different cell types with the loss of sacsin, raise the hypothesis that sacsin is involved in regulating IF dynamics. Through analyses of the effects of individual sacsin domains on NF assembly and resolution of abnormal NF bundles in *Sacs*$^{-/-}$ neurons, we showed that sacsin is crucial for normal NF assembly and dynamics *in vivo*. We also report that upregulating HSPs in neurons can, in part, correct the NF bundling caused by the loss of sacsin.

MATERIALS AND METHODS

Antibodies and reagents

Primary antibodies used for immunoblotting were as follows: mouse monoclonal anti-NFH antibody clone N52 (N0142, 1:400; MilliporeSigma, Burlington, MA, USA); mouse monoclonal anti-NFM antibody clone NN18 (N5254, 1:400; MilliporeSigma), mouse monoclonal anti-NFL antibody clone NR4 (N5139, 1:400; MilliporeSigma), mouse monoclonal anti–α-internexin antibody (clone 2E3, MAB5224, 1:400; Chemicon at MilliporeSigma), mouse monoclonal anti-flag antibody clone M2 (F3165, 1:400; MilliporeSigma), mouse monoclonal anti-HSPA1A (SPA810; Enzo Life Sciences, Farmingdale, NY, USA), rabbit polyclonal anti-peripherin (AB1530, 1:400; Abcam, Toronto, ON, Canada), mouse monoclonal anti-myc (clone 9E10, 1:400; Santa Cruz Biotechnology, Santa Cruz, CA, USA), goat polyclonal anti-myc (A14, 1:400; Santa Cruz Biotechnology), and rabbit polyclonal anti-acetyl-lysine (9441L, 1:1000; Cell Signaling Technology, Danvers, MA, USA). Peroxidase AffiniPure donkey anti-mouse and anti-rabbit IgG (715-035-150 and 711-035-152, 1:5000), Cy2-conjugated (715-225-151, 1:500), Cy3-conjugated (715-165-151, 1:500), donkey anti-mouse IgG and Cy3-conjugated (705-165-147), and donkey anti-goat IgG were from Jackson ImmunoResearch Laboratories (West Grove, PA, USA). Celastrol was from MilliporeSigma (C0869).

Plasmids

C terminus myc-tagged sacsin domains were constructed in pcDNA4.1 (NorClone Biotech Laboratories, London, ON, Canada) from pEGFP–sacsin full length (OriGene Technologies, Rockville, MD, USA): UBL (Sacs$^{aa\ 1-84}$), SIRPT1 (Sacs$^{aa\ 84-1374}$), SIRPT2 (Sacs$^{aa\ 1444-2443}$), or SIRPT3 (Sacs$^{aa\ 2512-4282}$), SacsJ (Sacs$^{aa\ 4316-4420}$), and HEPN (Sacs$^{aa\ 4422-4579}$). PcDNA mouse NFL, pRC-RSV rat NFH, and pcDNA HSP70 (HSPA1A) were previously described (27). pxcTRE-GFP-NFH was a gift from Dr. George Smith (Temple University, Philadelphia, PA, USA). *Nefh* CRISPR/cas9 knockout plasmid was from Santa Cruz Biotechnology (sc436192).

Cell culture

SW13^{vim-} cells, which lack endogenous IFs, were cultured in DMEM with 5% fetal bovine serum. Control fibroblasts were from the CellBank Repository for Mutant Human Cell Strains (McGill University Health Centre, Montreal, QC, Canada). ARSACS patient fibroblasts carrying the homozygous 8844delT mutation were previously described (9). Immortalized fibroblasts were cultured in DMEM with 5% fetal bovine serum. Cells were transfected with Lipofectamine 2000 in Opti-Mem (Thermo Fisher Scientific, Waltham, MA, USA) according to the manufacturer's instructions.

Primary cultures of dissociated spinal cord DRG were prepared from E13 *Sacs*$^{+/+}$ and *Sacs*$^{-/-}$ mice (C57Bl6 background). Generation and characterization of the *Sacs*$^{-/-}$ mice were as previously described (7); wild-type (*Sacs*$^{+/+}$) mice on the same background were used as control (*Sacs*$^{+/+}$). Cultures were plated on glass coverslips (Thermo Fisher Scientific) coated with poly-D-lysine (P7280; MilliporeSigma) and Matrigel (CACB354234; VWR, Mont-Royal, QC, Canada) and maintained in Eagle's Minimum Essential Medium (Thermo Fisher Scientific) enriched with 5 g/L glucose and supplemented with 3% horse serum, and other growth factors as previously described (38). Cultures were used in experiments 3–6 wk after plating to allow neuronal maturation. Motor neurons in long-term primary spinal cord cultures are not transfectable with lipophilic agents, and thus

plasmids were expressed by intranuclear microinjection at a concentration that resulted in detection of the encoded protein by immunocytochemistry in at least 90% of injected cells after 48 h. Plasmids encoding myc-tagged UBL ($Sacs^{aa\ 1-84}$), SIRPT1 ($Sacs^{aa\ 84-1374}$), SIRPT2 ($Sacs^{aa\ 1444-2443}$), SIRPT3 ($Sacs^{aa\ 2512-4282}$), SacsJ ($Sacs^{aa\ 4316-4420}$), and HEPN ($Sacs^{aa\ 4422-4579}$) were microinjected at 20 μg/ml. The CRISPR/Cas9 system was used to knockout *Nefh* gene expression in 3-wk-old cultured murine motor neurons using intranuclear injection of plasmids encoding Cas9, *Nefh* target sequences (or scramble), and EGFP to identify injected neurons.

Immunocytochemistry and electron microscopy

Cells were fixed with 4% paraformaldehyde in PBS added directly to the cultures after removing the culture medium. After incubation at 37°C for 30 min, cells were permeabilized with 0.3% Triton X-100 in 4% paraformaldehyde in PBS for 5 min at room temperature. Cells were washed with Tris-buffered saline (TBS) and blocked with 5% fetal bovine serum in TBS for 20 min. Cells were incubated with appropriate primary antibodies for 1 h. After a wash in TBS 3 times for 10 min, cells were incubated with secondary antibodies for 45 min, washed 3 times in TBS, and mounted in Immunomount (Thermo Fisher Scientific). Cells were observed by spinning confocal microscopy [Olympus IX81 (Richmond Hill, ON, Canada) with a Andor/Yokogawa spinning disk system (CSU-X), sCMOS camera, and ×100 or 60 objective lenses (NA1.4)]. Three-dimensional reconstruction of z-stack images and Pearson *R* values were obtained by using ImageJ software (National Institutes of Health, Bethesda, MD, USA; *https://imagej.nih.gov/ij/*). Cells were washed in PBS buffer and fixed with 2.5% glutaraldehyde (Electron Microscopy Sciences, Hatfield, PA, USA) in 0.1 M Na cacodylate buffer overnight at 4°C. Embedding and cutting were performed by the Facility for Electron Microscopy Research of McGill University. Briefly, cells were incubated in 1% osmium tetroxide (Mecalab, Barueri, São Paulo, Brazil) for 1 h at 4°C, and washed with ddH_2O 3 times for 10 min. Dehydration in a graded series of ethanol/deionized water solutions was then performed. Cells were gradually embedded with Epon 812 and polymerized overnight in an oven at 60°C. Polymerized blocks were trimmed and 100 nm ultrathin sections were cut with an UltraCut E Ultramicrotome (Jeannie Mui, Facility for Electron Microscopy Research, McGill University) and transferred onto 200-mesh Cu grids (Electron Microscopy Sciences). Sections were stained for 8 min with 4% aqueous uranyl acetate (Electron Microscopy Sciences) and 5 min with Reynold's lead citrate (Thermo Fisher Scientific). The data were collected on an FEI Tecnai-12 transmission electron microscope (Thermo Fisher Scientific) located at the Facility for Electron Microscopy Research at McGill University.

The range in the number of cells analyzed per condition is presented in the figure legends. For each experiment, a minimum 3 coverslips per condition from at least 2 culture batches were used to account for culture variability. IF bundling was scored according to the pattern of distribution in neurons labeled with anti-NFH or in fibroblasts by anti-vimentin. Scoring by 2 independent investigators was not statistically different (Student *t* test, unequal variance, $P = 0.081$). To examine the effect of sacsin domains on preexisting NF bundles, only neurons with bundles visible by phase contrast microscopy were microinjected (Supplemental Fig. S1).

Fluorescence recovery after photobleaching

Cultured $Sacs^{+/+}$ and $Sacs^{-/-}$ motor neurons were microinjected in the nucleus with plasmid encoding pXTRE-GFP-NFH (20 mg/ml). Twenty-four hours after injection, cultures were placed in a quick-release imaging chamber (QR41LP; Warner Instruments, Hamden, CT, USA) with neuronal culture medium (see Cell culture section) without red phenol and equilibrated 30 min at 37°C with 4% CO_2 in the incubation chamber of the spinning disk confocal microscope. Fluorescence recovery after photobleaching (FRAP) experiments were conducted by using an inverted IX81 microscope coupled with the FV1000 confocal scanning microscope (Olympus). Regions of interest in motor neurons expressing GFP-NFH were excited with the 488 nm laser. Images were continuously recorded until the fluorescence intensity in the bleached regions of interest (5 × 5 μm) reached plateau (imaged every 10 min for 140 min). Image and data acquisition was performed by using MetaMorph software (Universal Imaging, CA, USA). Intensity of fluorescence in the photobleached regions of interest at each time point was measured with MetaMorph software (Molecular Devices, Sunnyvale, CA, USA) and then expressed as a percentage of fluorescence intensity before photobleaching.

Statistics

Results of quantitative assays are expressed as means ± SD. Experiments reporting percentage of cells were performed from 2 separate culture batches; minimum and maximum numbers of cells per sample analyzed are indicated in brackets. Statistical analysis was performed by using 1-way ANOVA with a Tukey's honestly significant difference (HSD) *post hoc* analysis using GraphPad Prism (GraphPad Software, La Jolla, CA, USA) or MS Excel (Microsoft Corp., Redmond, WA, USA). Values of $P < 0.05$ were considered statistically significant.

All protocols were performed according to the guidelines of the Canadian Council on Animal Care and approved by the McGill University Animal Care Committee.

RESULTS

Loss of sacsin leads to bundling of NFs composed of multiple NF proteins

NF bundles have been detected by immunolabeling with antibody against NFH *in situ* in brain and spinal cord sections of $Sacs^{-/-}$ mice and in cultured spinal motor neurons and DRG neurons derived from these mice (7). NFs are heteropolymers requiring a core NF protein (NFL or peripherin, as well as α-internexin in development) to assemble with NFH and NFM (39–42). Thus, we assessed whether the bundled NFs in $Sacs^{-/-}$ neurons contained the normal complement of NF proteins, using dissociated spinal cord DRG cultures established from E13 $Sacs^{+/+}$ or $Sacs^{-/-}$ mice as control. NFL, NFM, NFH, peripherin, and α-internexin were all detected according to indirect immunocytochemistry in the NF bundles forming in motor neurons of 3-wk-old cultures, as well as normally distributed NFs in $Sacs^{-/-}$ and $Sacs^{+/+}$ neurons (**Fig. 1*A***).

The ultrastructure of NF bundles was examined by using transmission electron microscopy of 6-wk-old $Sacs^{+/+}$ (Fig. 1*B*) and $Sacs^{-/-}$ (Fig. 1*C*) cultures. Fig. 1*C* illustrates a $Sacs^{-/-}$ motor neuron with bundles of densely packed NFs extending from around the nucleus and coursing through a dendritic process, in contrast to the more sparsely distributed network in the $Sacs^{+/+}$ neuron shown in Fig. 1*B*. The enlargement in Fig. 1*C* shows extensive cross-bridging

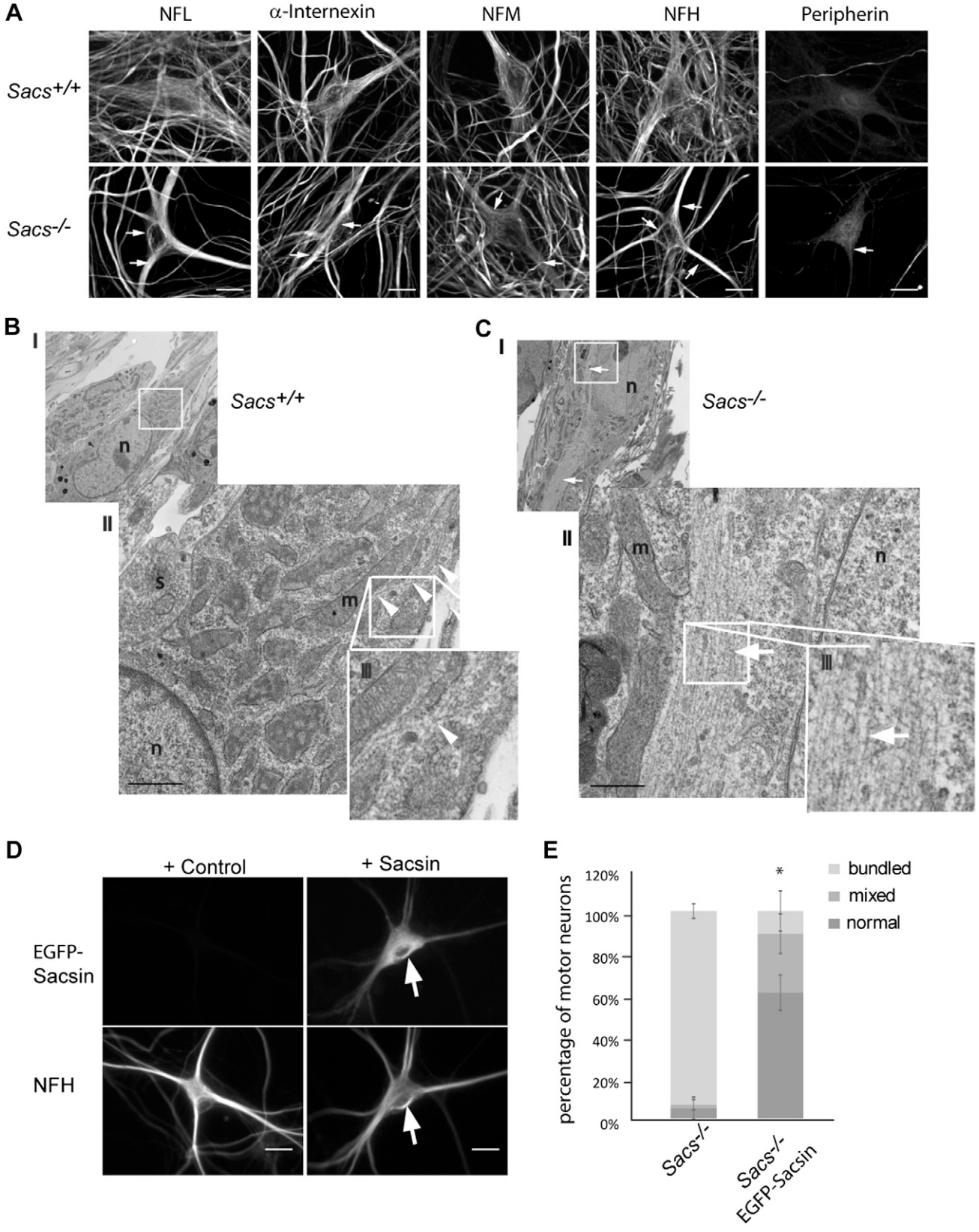

Figure 1. *A*) Loss of sacsin induces bundling of NF containing multiple NF proteins. Representative images of motor neurons in 3-wk-old dissociated spinal cord DRG cultures established from $Sacs^{+/+}$ (upper panel) and $Sacs^{-/-}$ (lower panel) mice immunolabeled for distribution of the NF proteins NFL, α-internexin, NFM, NFH, and peripherin, showing labeling in NF bundles (arrows). Peripherin expression is low at this stage of development in $Sacs^{+/+}$ cultures but is more persistent in $Sacs^{-/-}$ neurons, as previously reported (7). Scale bars, 10 μm. *B, C*) Representative electron microscopy images of motor neurons in 6-wk-old dissociated spinal cord DRG cultures established from $Sacs^{+/+}$ (*B*) and $Sacs^{-/-}$ (*C*) mice showing typical cytoskeleton (*B,*

(*continued on next page*)

between the parallel arrays of NFs in the *Sacs*$^{-/-}$ neuron. Organelles including mitochondria were sparse within dense NF bundles, being largely excluded to the periphery, consistent with our previous observations at the light microscopic level in cultured motor neurons (8). From an ultrastructural point of view, bundles in *Sacs*$^{-/-}$ motor neurons are made of juxtaposed NF. Thick NF bundles in *Sacs*$^{-/-}$ neurons often course through the neuronal cell body from one dendrite to another (Fig. 1*A*). They are distinguished from small bundles of NFs that normally occur in neurons. They also differ from the NF bundles described by others that are enriched in phosphorylated NFH and immunoreactive with monoclonal antibody RT97 (43, 44) in being hypophosphorylated (7).

Ectopically expressed sacsin decorates and resolves NF bundles in *Sacs*$^{-/-}$ motor neurons

We next assessed whether NF bundling was reversible by ectopically expressing wild-type sacsin. These bundles were visible in living cultures according to positive-phase contrast microscopy as thick bright bands coursing through motor neuronal cell bodies and joining 2 opposite dendrites (Supplemental Fig. S1); thus, sacsin could be expressed exclusively in neurons with preexisting bundles. Plasmid encoding full-length sacsin tagged with EGFP was microinjected into motor neurons with bundles in 6-wk-old *Sacs*$^{-/-}$ spinal cord DRG cultures using an empty plasmid as a control. After 2 d, cultures were fixed and double-labeled with antibody to NFH as the NF marker. EGFP-sacsin decorated NF bundles labeled by anti-NFH, indicating an intimate association (Fig. 1*D*). Expression of sacsin also significantly diminished the number of neurons with significant NF bundling compared with motor neurons in sister cultures microinjected with empty plasmid, as determined by the NFH immunolabeling (see Materials and Methods) (Fig. 1*E*). At 2 d, NF bundling was most resolved in the cell body of motor neurons relative to dendrites. Thus, some sacsin colocalizes with NF and NF bundles in sacsin null cells (Pearson *R* value = 0.8). Moreover, expressing full-length sacsin leads to variable resolution of NF bundling, indicating that the process is reversible and further supporting the putative role of sacsin in regulating NF dynamics.

NFH turnover is slowed in NF bundles

To obtain more information on the stability and subunit turnover in NF bundles in *Sacs*$^{-/-}$ motor neurons, NFH was knocked down by coexpression of plasmids encoding EGFP-CRISPR/Cas9 and a set of *Nefh*-targeting guide RNA (gRNA), specifically in neurons with NF bundles visible by phase microscopy. After 3 d, the cultures were fixed, and targeted motor neurons were identified according to EGFP epifluorescence. The expression of endogenous NFH was detected and quantified by fluorescence intensity of immunolabeling by using the N52 monoclonal phospho-independent NFH antibody. *Sacs*$^{-/-}$ motor neurons expressing scrambled gRNA retained NFH and NFH-containing bundles (**Fig. 2*A***), whereas NFH was depleted from cell bodies and dendrites of neurons expressing the *Nefh*-targeting gRNA (Fig. 2*B*). Therefore, NFH previously incorporated into NF bundles was removed over time. Despite arrest of NFH expression, NF bundles comprising other NF proteins were still present in cells in which *Nefh* was targeted, detected by antibody against the NF core protein NFL (Fig. 2*C*, *D*), indicating that NFH turns over in NF bundles in *Sacs*$^{-/-}$ neurons.

The rate of NFH turnover in bundled and nonbundled NF was evaluated by using FRAP experiments. EGFP-NFH was expressed in motor neurons of *Sacs*$^{+/+}$ or *Sacs*$^{-/-}$ spinal cord DRG cultures by intranuclear microinjection. After 3 d, small regions of incorporated EGFP-NFH were photobleached in cell bodies (**Fig. 3*A***) and axons (Fig. 3*B*). Recovery of the fluorescence in the region, reflecting subunit exchange by unbleached subunits (45), was quantified over time. Fluorescence recovery was decreased relative to *Sacs*$^{+/+}$ neurons only within NF bundles in *Sacs*$^{-/-}$ motor neuronal cell bodies and axons, not in neurons with normally distributed NF, as shown by the increase in the immobile NFH fraction (mean ± SD, 60 ± 4.13% in *Sacs*$^{-/-}$ axons with bundles *vs.* 34 ± 6.3% in *Sacs*$^{-/-}$ axons without bundles *vs.* 30 ± 3.24% in *Sacs*$^{+/+}$ axons). These results show that NFH turnover still occurs in the absence of sacsin but is impaired only in bundled NF, implying a secondary, rather than primary, defect, perhaps due to impaired access of necessary factors into the packed NF.

Individual sacsin domains have different effects on NF assembly, organization, and turnover

To gain further insight into the role of the predicted individual functional domains of sacsin on NF dynamics, we first examined their influence on *de novo* assembly of NF by using SW13^{vim-} cells, a conventional model for studying assembly of NF proteins because they lack endogenous IFs (46). Plasmids encoding myc-tagged sacsin domains, shown in **Fig. 4*A***, were generated and coexpressed with NFL and NFH, NF proteins that together form NFs arranged in a network coursing through the cell (Fig. 4*B*

arrow head) and NF bundles (*C*, arrows). Middle panel (*II*) is a magnification of the region identified by the white square in the upper panel (*I*); lower panel (*III*) is a 3× magnification of the region identified by the white square in the upper panel (*II*). n, neuronal nucleus; m, mitochondria; s, synapse. Scale bars, 500 nm. *D*) Resolution of NF bundles in neurons ectopically expressing full-length sacsin. Representative three-dimensional reconstitution of z-stack confocal images of 6-wk-old *Sacs*$^{-/-}$ motor neurons without (empty plasmid as control, left) or with ectopic expression of EGFP-sacsin (right). Bottom panels: double label of neurons expressing EGFP-sacsin with antibody against NFH to reveal NF distribution in the same cells. Arrow points to codistribution of sacsin with a perikaryal NFH bundle. Scale bars, 10 μm. *E*) Quantitation of the effect of EGFP-sacsin on the presence of NF bundles in *Sacs*$^{-/-}$ motor neurons as the percentage of neurons exhibiting a normal NF network, NF bundles, or mixed (normal network in the cell body and bundling in the dendrites). *$P < 0.05$ *vs.* control ($n = 3$, 20–30 neurons/coverslip) Tukey's HSD *post hoc* analysis.

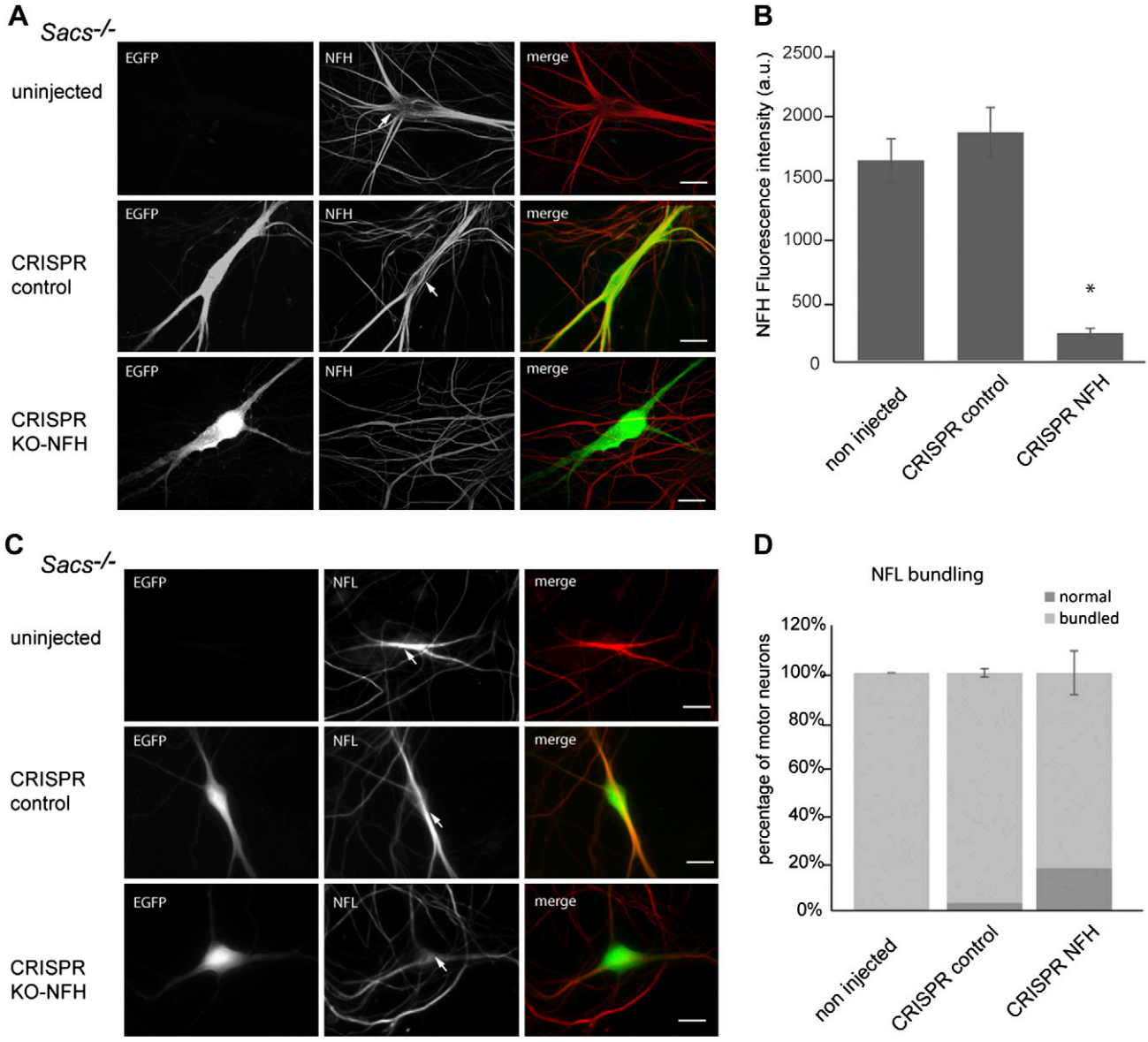

Figure 2. NFH turns over in NF bundles in $Sacs^{-/-}$ motor neurons. *Nefh* knockout was accomplished by using the CRISPR/Cas9 system in motor neurons of 6-wk-old spinal cord DRG cultures. Only motor neurons with NF bundles visible according to phase microscopy were microinjected with plasmids encoding EGFP-CRISPR/Cas9 and a set of gRNA targeting *Nefh*. EGFP encoded by the CRISPR/Cas9 plasmid was used to identify microinjected cells. *A*) After 2 d, cultures were fixed and immunolabeled by N52 antibody against NFH. Shown are representative images with arrows pointing to NF bundles in control (uninjected or injected with nonspecific gRNA sequences). NFH was depleted from almost all neurons expressing *Nefl* gRNA, including from the bundles. Scale bars, 10 μm. *B*) Quantitation of fluorescence intensity in arbitrary units (a.u.) of anti-NHF immunolabeling in noninjected motor neurons with bundles, or injected with plasmids encoding CRISPR/Cas9 with control (nonspecific) or Nefh-targeting sequences. $*P < 0.05$ *vs.* control, $n = 10$, 1-way ANOVA with Tukey's HSD *post hoc* analysis. *C*) Bundles containing NFL remain after depletion of NFH. Representative confocal images of NFL immunolabeling (NR4 mouse mAb) in noninjected $Sacs^{-/-}$ motor neurons or $Sacs^{-/-}$ motor neurons expressing control gRNA or gRNA targeting NFH. *D*) The percentage of motor neurons with bundles labeled by anti-NFL was not significantly different under the experimental conditions described for NFH knockout. Scale bars, 10 μm. $P > 0.05$, 1-way ANOVA with Tukey's HSD *post hoc* analysis.

and Supplemental Fig. S2). Cells were classified according to the predominance of 4 different phenotypes observed (short filaments, long filaments, diffuse, or bundled/aggregated filaments) (Fig. 4C). UBL domain–containing proteins are typically involved in regulating protein turnover by associating substrates targeted for degradation with the proteasome (47). Ectopic expression of the myc-tagged sacsin UBL domain resulted in the formation of oligomeric structures and shorter filaments of various sizes throughout the cell. Expression of the SacsJ domain also inhibited NFL/NFH assembly and the formation of an NF network in the cell. The short fragments produced were diffusely spread throughout the cell, resembling filament precursors (13). Ectopic expression of the myc-tagged sacsin SIRPT domains, containing a domain homologous to the ATP-binding domain of HSP90, induced the formation

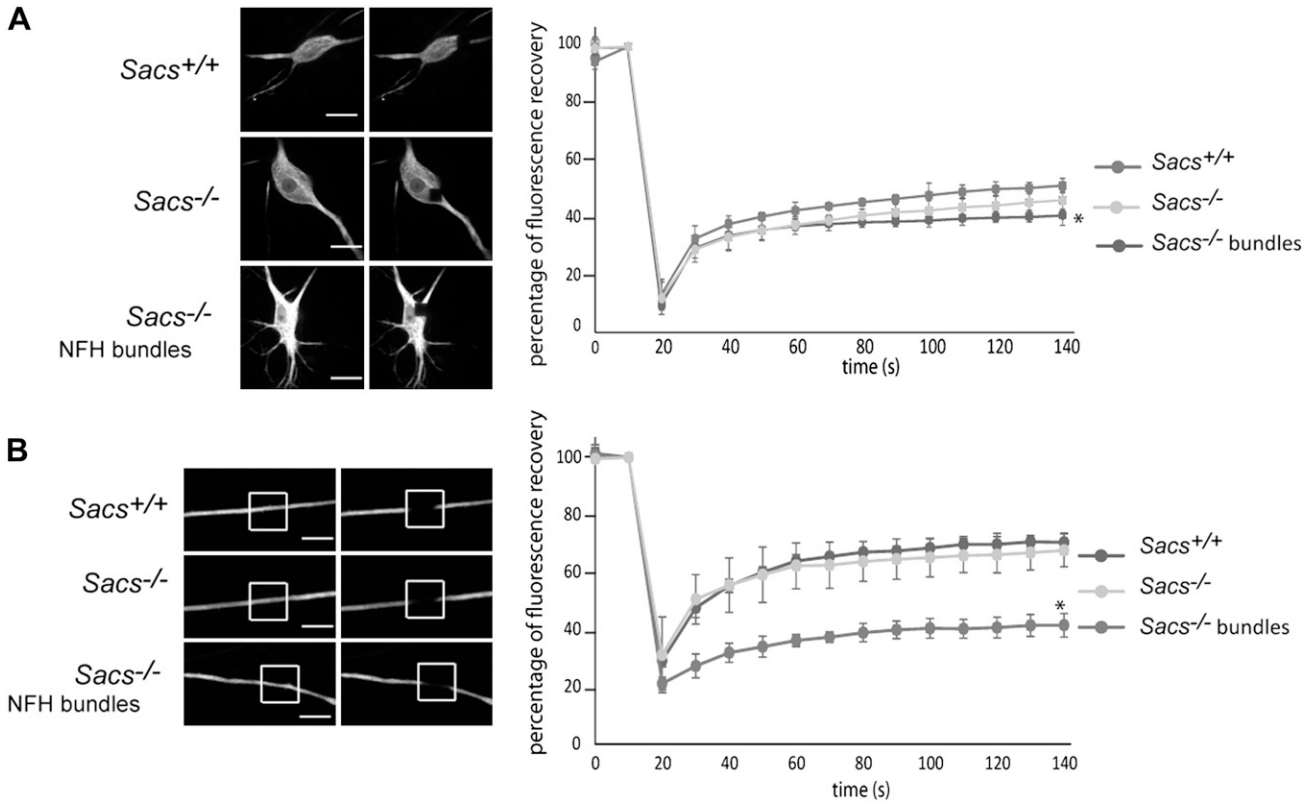

Figure 3. The rate of turnover of NFH is reduced but only in NF bundles in $Sacs^{-/-}$ motor neurons. NFH turnover and transport were assessed by using FRAP in cell bodies (*A*) and axons (*B*) of motor neurons expressing EGFP-tagged NFH. Left panels: Representative confocal images showing the regions selected for FRAP in cell body (*A*) or axonal segments (*B*) of cultured $Sacs^{+/+}$ and $Sacs^{-/-}$ motor neurons expressing EGFP-NFH, before and immediately after photobleaching. Scale bars, 20 (*A*) and 5 (*B*) μm. Right panel: Graphical representation of FRAP in $Sacs^{+/+}$ and $Sacs^{-/-}$ motor neurons with or without NF bundles according to time after photobleaching, showing that the immobile fraction was increased in $Sacs^{-/-}$ cell bodies with bundles relative to unbundled NF in those cultures and NF in $Sacs^{+/+}$ neurons (n = 3, 20–32 neurons/coverslip), $^*P < 0.05$, 1-way ANOVA with Tukey's HSD *post hoc* analysis.

of long, fine filament arrays; however, SIRPT1 was more efficient in promoting the formation of long filaments. Finally, with expression of the HEPN domain, NFL and NFH formed long filaments arranged in a cage-like structure at the periphery of the cell (see three-dimensional reconstruction in Supplemental Fig. S3*A*, *B*). Thus, the UBL and SacsJ domains had an overall inhibitory effect on establishing a *de novo* NF network, whereas the SIRPT and HEPN domains promoted NF formation and networking.

To determine how replacement of individual sacsin domains would affect already established NF bundles in sacsin-deficient neurons, myc-tagged sacsin domains were expressed by intranuclear microinjection of plasmid expression vector into motor neurons in 6-wk-old $Sacs^{-/-}$ spinal cord DRG cultures, specifically in those neurons in which NF bundles were visible by phase microscopy (Supplemental Fig. S1). Expression of sacsin domains was detected by anti-myc immunolabeling, and NF bundles were visualized and evaluated by double-labeling cells with anti-NFH (**Fig. 5*A, B*** and Supplemental Fig. S4). Three days after microinjection, fewer neurons expressing myc-tagged UBL, SIRPT1, or SacsJ had NFH bundles; however, expression of the SIRPT2, SIRPT3, and HEPN domains had no or minimal effect. The SacsJ domain was the most efficient in resolving NF bundles. The UBL domain was less efficient, with NFH-containing bundles often remaining in the dendrites at this time (Fig. 5*A*, arrow).

Qualitatively, the effect of sacsin domains on assembly of NF in $SW13^{vim-}$ cells and on preexisting NF bundles in motor neurons was consistent, the exception being SIRPT1, which promoted *de novo* formation of long filaments but also reduced NF bundling in neurons lacking sacsin (Fig. 5*B*).

Absence of sacsin also causes bundling and juxtanuclear collapse of IFs composed of vimentin in cultured fibroblasts derived from patients' skin biopsy specimens (8). We determined the effects of sacsin UBL, SIRPT1, SacsJ, and HEPN domains on IF organization in a fibroblast line homozygous for the loss-of-function 8844delT sacsin mutation resulting in loss of sacsin expression and bundling of vimentin IFs (Supplemental Fig. S5). Ectopic expression of the different sacsin domains had no significant effect on the IF network in control fibroblasts; however, expression of either SIRPT1 or SacsJ reduced the percentage of ARSACS fibroblasts with juxtanuclear IF bundles as they did for NF bundles in $Sacs^{-/-}$ motor neurons. Qualitatively, expression of SIRPT1 induced the formation of a long, reticulated vimentin network with cell enlargement, and expression of SacsJ disassembled the vimentin

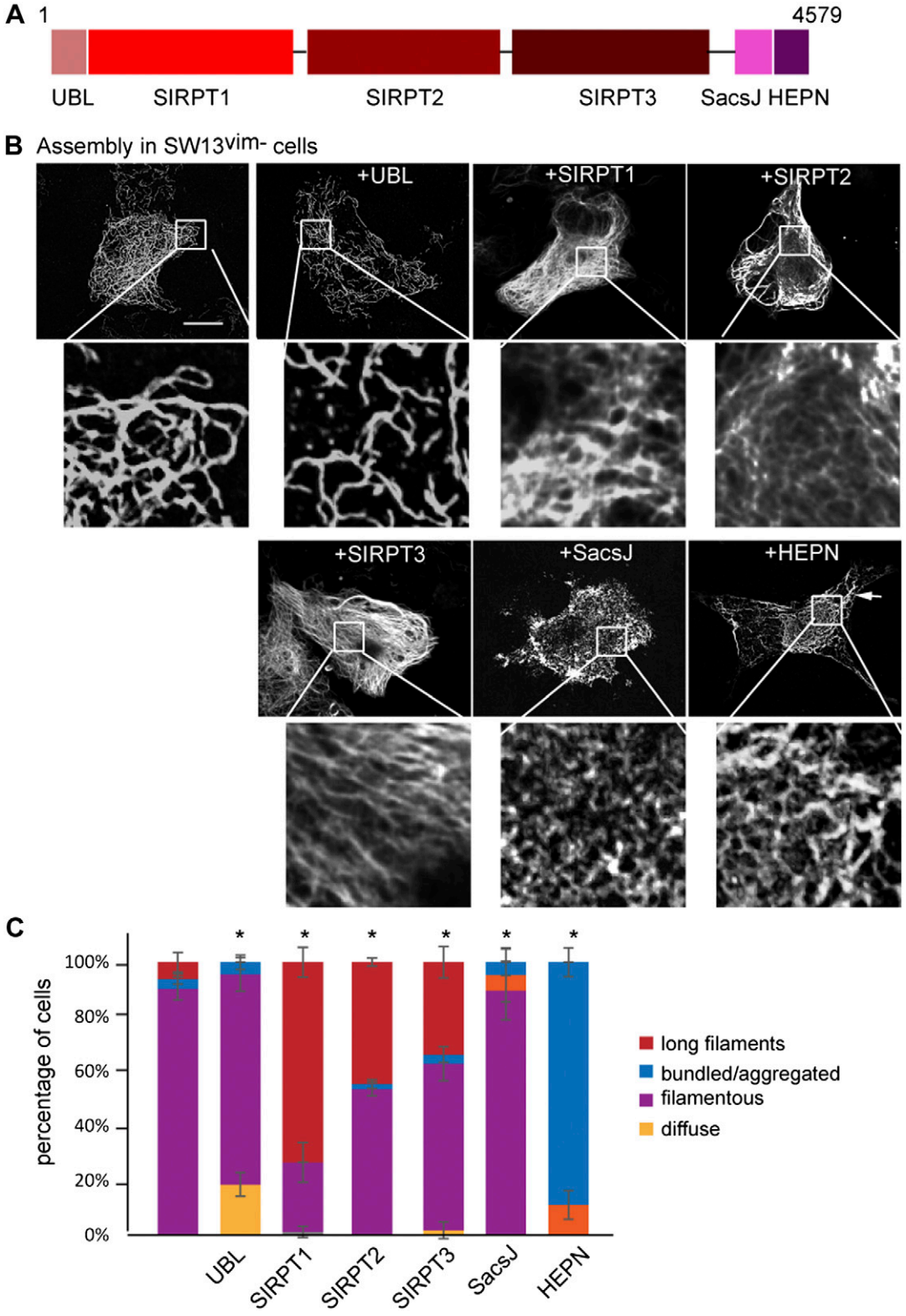

Figure 4. Effect of sacsin domains on *de novo* NF assembly. *A*) Representation of sacsin domains. Sacsin bears several putative functional domains identified *in silico*, and C-terminal myc-tagged constructs corresponding to these domains were used in this study: UBL ($Sacs^{aa\ 1-83}$), SIRPT1 ($Sacs^{aa\ 84-1374}$), SIRPT2 ($Sacs^{aa\ 1444-2443}$), or SIRPT3 ($Sacs^{aa\ 2512-4282}$), SacsJ ($Sacs^{aa\ 4316-4420}$), and HEPN ($Sacs^{aa\ 4422-4579}$). *B*) The effect of these sacsin domains on *de novo* NFL/NFH assembly into filamentous structures was assessed in $SW13^{vim-}$ cells (which lack endogenous IFs). Cells were cotransfected with plasmids encoding NFL, NFH, and one of the sacsin domains. Expression of the sacsin domain was confirmed by double-immunolabeling with anti-myc, and NFs were detected with monoclonal anti-NFH (clone N52). Representative three-dimensional reconstructions of *z*-stack confocal images of the NF network in cells coexpressing NFL and NFH or together with the sacsin UBL, SIRPT1, SIRPT2, SIRPT3, SacsJ, or HEPN domain. The UBL domain promoted formation of shorter filaments of variable length but did not prevent NF assembly. SIRPT

(*continued on next page*)

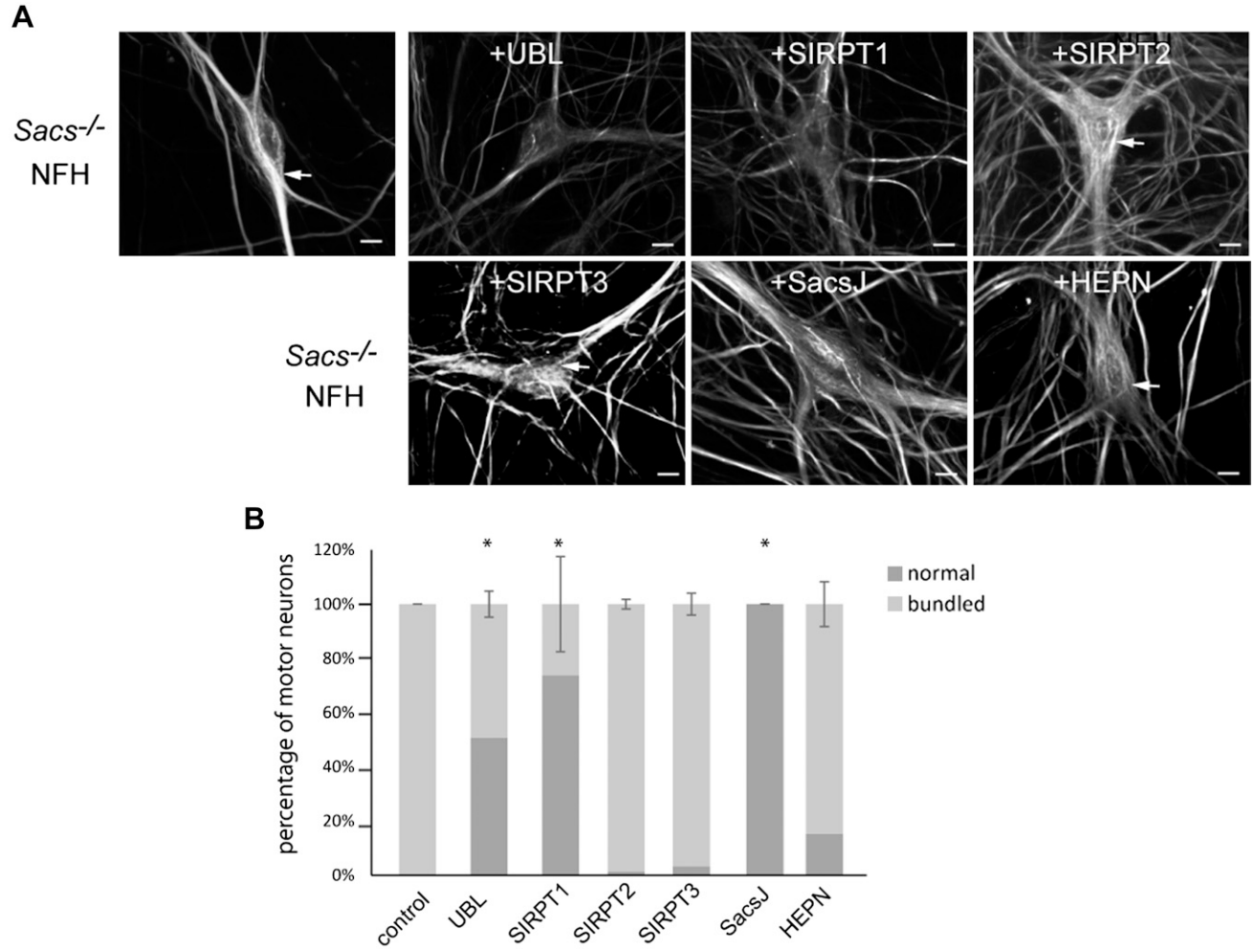

Figure 5. Effect of sacsin domains on preexisting NF bundles in *Sacs*$^{-/-}$ motor neurons (arrows). *A*) Three-dimensional reconstructions of the NF network in motor neurons of 6-wk-old dissociated cultures of *Sacs*$^{-/-}$ spinal cord DRG. Shown are representative images 3 d after intranuclear microinjection of empty plasmid or plasmid encoding myc-tagged UBL, SacsJ, HEPN, SIPRT1, SIRPT2, or SIRPT3 sacsin domains. Expression of the sacsin domain was visualized by anti-myc immunolabeling. The NF network was assessed by double-labeling with anti-NFH. Expression of the UBL domain induced general down-regulation of NFH expression and resulted in fewer bundles. Of the SIRPT domains, only SIRPT1 resulted in a very reticulated filamentous network of fine filaments. In the presence of the SacsJ domain, NF bundles were essentially resolved. The HEPN domain did not significantly affect NF bundles. Scale bars, 10 μm. *B*) Quantitation of the effect of ectopic expression of sacsin on the percentage of cultured *Sacs*$^{-/-}$ motor neurons with NF bundles. Expression of UBL, SIRPT1, and SacsJ efficiently reduced the proportion of motor neurons with bundled NF, with the HEPN domain having minimal effect. *$P < 0.05$ *vs.* control, 1-way ANOVA Tukey's HSD *post hoc* analysis ($n = 3$, 15–50 neurons/coverslip).

bundles. Taken together, the results support sacsin playing an important role in IF organization and dynamics.

Up-regulating molecular chaperones partially compensates for sacsin loss of function in NF organization

The partial resolution of NF bundles in *Sacs*$^{-/-}$ motor neurons by expression of its J-domain suggests that sacsin acts in the chaperoning of NF proteins. HSPs, including the stress-inducible human HSP70-1 isoform, HSPA1A, are known to influence solubility of IFs and can, when overexpressed, correct NF abnormalities in other neurologic disorders, including rare forms of Charcot-Marie-Tooth disease (27, 48). SacsJ domain was shown to have some minimal chaperone function (34) and also bears homology to the DNAJ/Hsp40 protein chaperone, a cofactor for ATP-dependent folding of Hsp70 substrates, among others. Therefore, we explored

domains promoted formation of a reticulated filamentous network of fine filaments. In the presence of the SacsJ domain, NFL and NFH formed small and dispersed oligomeric structures. The HEPN domain promoted formation of thicker NF bundles (arrow) that organized into a cage-like structure visible in optical sections (Supplemental Fig. S4). Scale bar, 10 μm. *C*) Quantitation of the different NF phenotypes observed in *B* expressed as a percentage of motor neurons coexpressing the various sacsin domains. Phenotypes were described depending on NF length, long filaments (≥40 μm), bundled/aggregated (≥20 μm), and bright (see arrow in *B*), filamentous (10 μm ≤ and ≤ 40 μm), and diffuse (≤10 μm). *$P < 0.05$ *vs.* control ($n = 3$ cultures, 40–100 cells/coverslip), 1-way ANOVA Tukey's HSD *post hoc* analysis.

whether the effect of increasing expression of HSPA1A could modify NF bundling in *Sacs*$^{-/-}$ cultured motor neurons. Although motor neurons express high levels of constitutive Hsc70 and Hsp70 isoforms, they are resistant to up-regulation of this stress-inducible isoform (49, 50). HSPA1A was not up-regulated in 6-wk-old *Sacs*$^{-/-}$ or *Sacs*$^{+/+}$ motor neurons in culture (**Fig. 6*A***). However, ectopic expression of plasmid encoding HSPA1A resolved preexisting NF bundles by 3 d post-microinjection (Fig. 6*B*, *C*) with comparable efficiency as the SacsJ domain (Fig. 6*A*, *B*).

We also tested celastrol, a naturally occurring pentacyclic triterpenoid that induces expression of multiple HSPs, including HSPA1A, DNAJB1, and HSPB1 (51); HSPA1A was used as the marker of induction. Treatment with 1 μM celastrol for 24 h induced expression of HSPA1A in cultured *Sacs*$^{-/-}$ motor neurons and resolved NF bundles, as visualized by immunolabeling of NFH, in 83 ± 16% of motor neurons (mean ± SD) (Fig. 6*B*, *C*), indicating compensation for loss of sacsin function.

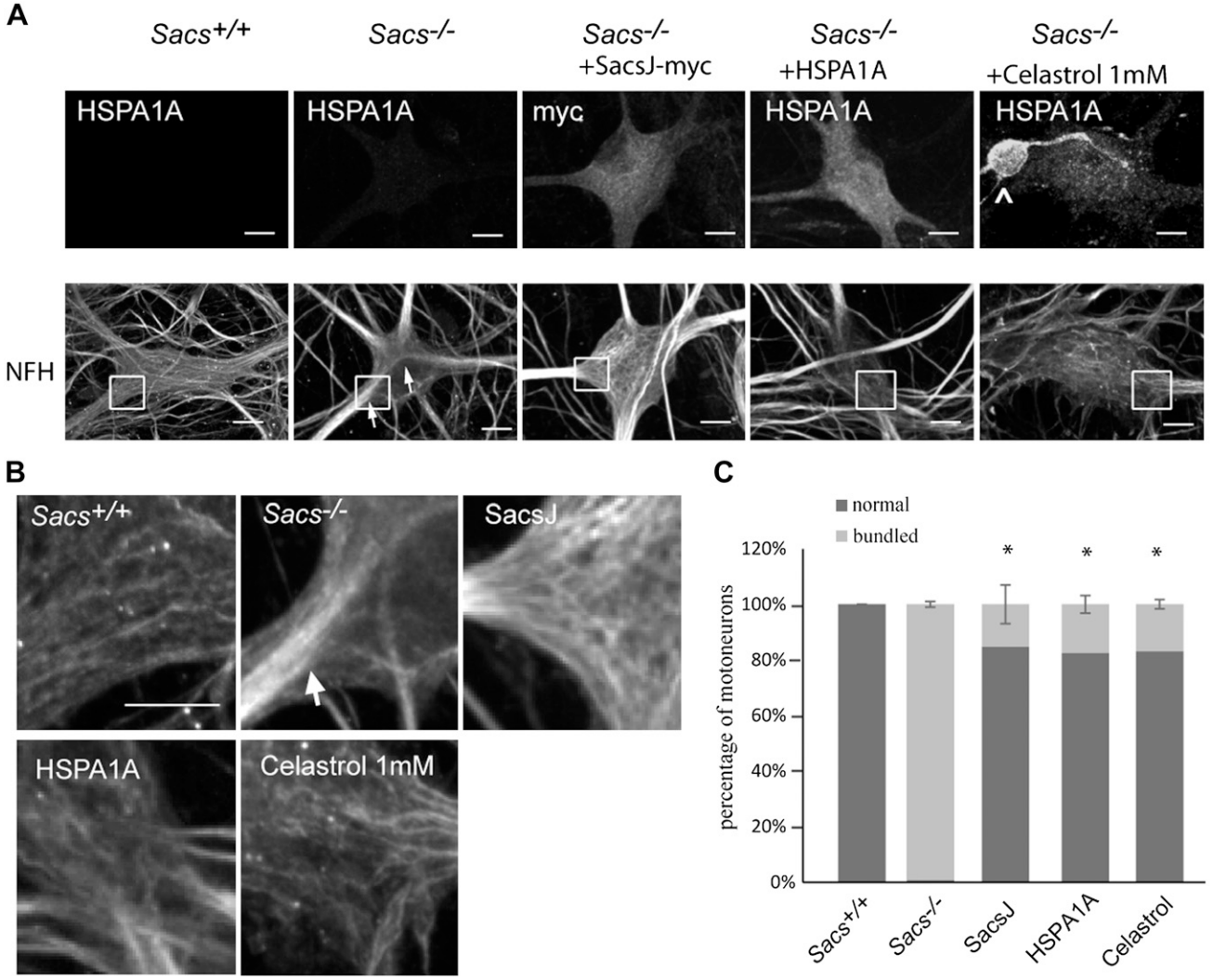

Figure 6. Increased HSP expression resolves NF bundles in *Sacs*$^{-/-}$ motor neurons. *A*) To induce chaperoning activity, HSPs were up-regulated by expression of the stress-inducible HSP70 isoform HSPA1A in *Sacs*$^{-/-}$ motor neurons by intranuclear plasmid microinjection or by treating cultures with the HSP-inducing drug, celastrol (1 mM). The effect on NF bundles in motor neurons was assessed by NFH immunolabeling and compared with expression of the SacsJ domain (see Fig. 5). For microinjection, motor neurons in 6-wk-old dissociated spinal cord DRG cultures (*Sacs*$^{-/-}$ and *Sacs*$^{+/+}$) were randomly microinjected with plasmid encoding sacsin SacsJ-Myc or human HSPA1A. Neurons were not preselected for bundles in this experiment; however, 95–100% of motor neurons at that stage presented bundles observable according to phase. Cells were fixed 2 d later and immunolabeled with anti-NFH and anti-HSPA1A. Representative image of NFH immunolabeling. Shown are representative images of motor neurons under the various conditions. Arrow points to high HSPA1A in a Schwann cell adjacent to a motor neuron (Schwann cell that reacted particularly well to HSP induction by celastrol). Scale bars, 10 μm. *B*) Higher power micrographs of the neuronal cell body showing NFH network presented as an enlargement of motor neurons shown in *A*. Scale bar, 10 μm. *C*) Quantitation of the effect of ectopic expression of the SacsJ domain or HSPA1A at 2 d after injection on NFH bundling in *Sacs*$^{-/-}$ motor neurons in culture or after 24 h treatment with celastrol 1 μM. It is noteworthy that the 3 experimental conditions resulted in similar resolution of NF bundling. *$P < 0.05$ *vs.* control (uninjected neurons), 1-way ANOVA Tukey's HSD *post hoc* analysis ($n = 3$, 11–66 motor neurons/coverslip).

DISCUSSION

Disruption of cytoskeletal structure and dynamics is linked to disease, with mutations in IF proteins or small HSP chaperones causing disorders with IF pathology (NFL, HSPB1, HSPB3, HSPB5, HSPB6, HSPB8, desmin, and keratins). The resulting diseases include sensorimotor neuropathies, myopathies, cataracts, and skin disorders (52, 53). The present study further establishes ARSACS as an IF disorder and implicates distinct, but complementary, functions of sacsin domains in IF organization and turnover.

Sacsin is a large protein with a C-terminal UBL domain, 3 SIRPT domains, a J-domain, and an N-terminal HEPN domain. To address the function of sacsin in regulating NF, we determined the effect of individual domains of sacsin on NF assembly *in vivo* and their effect on established bundles of NF in *Sacs*$^{-/-}$ neurons.

The domains with chaperone homology, SIRPT and J-domain, had opposite effects on *de novo* NF assembly in SW13^{vim-} cells (NFL and NFH), pointing to sacsin being a multifunctional protein. SIRPT1, homologous to the ATP-binding domain of HSP90, promoted the assembly of NFL and NFH into filamentous structures in SW13^{vim-} cells, which is consistent with the role of HSP90α1 in chaperoning myosin in thick filament precursors for ordered assembly (54, 55). We speculate that the organization in tandem of the 3 SIRPT domains of sacsin may facilitate this process by compacting longer NF stretches. Thus, sacsin through the SIRPT domains belongs to the class of assembly chaperones, which assist the assembly of folded proteins into larger mature structures (56–58). Conversely, the SacsJ domain prevented the assembly of NF in SW13^{vim-} cells, which is reminiscent of the role of Mrj, a DNAJ/HSP40 involved in disassembly of preexisting keratin IF (59). Because SacsJ has been described as a co-chaperone of HSP70 (34), the maintenance of this pool of nonfilamentous NFs could be seen as a canonical role of DNAJ proteins in client specificity and as a way to maintain NF quality control within the cell (60). The SacsJ domain behaved like other molecular chaperones (HSPB1, HSPB8, and αB-crystallin) that influence IF solubility in detergent, preventing them from forming filaments (29, 61).

UBL domain–containing proteins are typically involved in proteasomal degradation. The sacsin UBL domain reportedly binds to the proteasome (34). Coexpression of the UBL domain in SW13^{vim-} cells resulted in formation of short filaments of multiple lengths, indicating either failure of precursors to anneal to form longer filaments or severing of newly formed filaments.

Conversely, expression of the sacsin HEPN domain in SW13^{vim-} cells resulted in assembly of NFL and NFH into a cage-like structure around the cell periphery. Aside from binding nucleotides, little is known about the functions of HEPN domains (37). Anantharaman *et al.* (36) proposed that the sacsin HEPN domain might act either as an RNase or as a noncatalytic RNA-binding domain. Further investigation is necessary to determine if the HEPN domain of sacsin facilitates NF–RNA interaction.

The activity of sacsin's individual domains shown in this study point to sacsin as a gigantic "hub" functioning at multiple levels of NF biology, including regulating subunit levels, assembly, and maturation. The colocalization of ectopic EGFP-sacsin full length and domains with NF bundles in *Sacs*$^{-/-}$ neurons suggests that sacsin is a key player in organizing NF proteins into a filamentous network. The SIRPT1 and the SacsJ domains could potentially act cooperatively to fine-tune NF maturation into compact filaments, for turnover or control quality.

In *Sacs*$^{-/-}$ motor neurons, the FRAP experiments showed that turnover of NFH still occurred in the absence of sacsin, although more slowly in bundled NFs. Thus, failure of subunit turnover is not the major cause of NF bundling in *Sacs*$^{-/-}$ neurons. The reduced subunit turnover in bundled NF could be a secondary result of either a reduced access of factors regulating subunit exchange in densely packed filaments or of insufficient NF subunits or precursors available for assembly. Nevertheless, ectopically expressed sacsin, both the SIRPT1 and SacsJ domains, and to a lesser extent the UBL domain, resolved preexisting NF bundles, illustrating sacsin's importance in NF regulation. The co-localization of EGFP-sacsin with NF bundles in *Sacs*$^{-/-}$ neurons suggests a direct interaction with NFs.

Although NFs were the main focus of the present study, we also investigated the effect of sacsin domains on bundled vimentin IFs in immortalized fibroblasts derived from a skin biopsy specimen of a patient with ARSACS. Consistent with sacsin's role in regulating IFs in multiple cell types, the effects of sacsin domains were qualitatively similar in ARSACS fibroblasts and *Sacs*$^{-/-}$ neurons, with the SIRPT1, SacsJ, and UBL domains showing some ability to resolve both vimentin IF and NF bundles.

In terms of replacement therapy, as with other very large proteins such as dystrophin, defining the minimal functional construct amenable to packaging in delivery vehicles will be the next challenge. The domain analysis in this study paves the way for that design.

An alternative strategy is up-regulation of a relevant pathway to compensate for loss of sacsin function, namely up-regulation of HSP chaperones. Indeed, both ectopic expression of HSPA1A and treatment with the HSP inducer, celastrol, rapidly resolved NF bundles in culture *Sacs*$^{-/-}$ motor neurons. Inducers more amenable to therapeutic application are being investigated. FJ

ACKNOWLEDGMENTS

The authors thank Nicolas Sgarioto (Montreal Neurological Institute, McGill University) for the management of the *Sacs*$^{-/-}$ colonies. The authors thank Jeannie Mui and Dr. Vali (Facility for Electron Microscopy Research, McGill University) for help in microscope operation and data collection. This study was supported by grants from the Ataxia of Charlevoix-Saguenay Foundation (to H.D.D., B.B., K.G., and J.-P.C.) and Biotechnology and Biological Sciences Research Council (BBSRC) Grant BB/R003335/1 (to J.-P.C.). The authors declare no conflicts of interest.

AUTHOR CONTRIBUTIONS

B. J. Gentil and H. D. Durham conceived, designed, and supervised the project and wrote the manuscript, with key input from the other authors; G.-T. Lai performed and analyzed the expression of sacsin domains in fibroblasts;

B. J. Gentil performed all other experiments and analyzed the majority of the data; R. Larivière produced plasmids encoding SIRPT1, SIRPT2, and SIRPT3 domains; S. Minotti produced and maintained spinal cord cultures; B. Brais provided the *Sac*$^{-/-}$ mice and key input to the manuscript; and J.-P. Chapple, M. Menade, and K. Gehring provided key insights and suggestions for the experiments.

REFERENCES

1. Baets, J., Deconinck, T., Smets, K., Goossens, D., Van den Bergh, P., Dahan, K., Schmedding, E., Santens, P., Rasic, V. M., Van Damme, P., Robberecht, W., De Meirleir, L., Michielsens, B., Del-Favero, J., Jordanova, A., and De Jonghe, P. (2010) Mutations in SACS cause atypical and late-onset forms of ARSACS. *Neurology* **75**, 1181–1188
2. Bouchard, J. P., Barbeau, A., Bouchard, R., and Bouchard, R. W. (1979) Electromyography and nerve conduction studies in Friedreich's ataxia and autosomal recessive spastic ataxia of Charlevoix-Saguenay (ARSACS). *Can. J. Neurol. Sci.* **6**, 185–189
3. El Euch-Fayache, G., Lalani, I., Amouri, R., Turki, I., Ouahchi, K., Hung, W. Y., Belal, S., Siddique, T., and Hentati, F. (2003) Phenotypic features and genetic findings in sacsin-related autosomal recessive ataxia in Tunisia. *Arch. Neurol.* **60**, 982–988
4. Ouyang, Y., Segers, K., Bouquiaux, O., Wang, F. C., Janin, N., Andris, C., Shimazaki, H., Sakoe, K., Nakano, I., and Takiyama, Y. (2008) Novel SACS mutation in a Belgian family with sacsin-related ataxia. *J. Neurol. Sci.* **264**, 73–76
5. Ouyang, Y., Takiyama, Y., Sakoe, K., Shimazaki, H., Ogawa, T., Nagano, S., Yamamoto, Y., and Nakano, I. (2006) Sacsin-related ataxia (ARSACS): expanding the genotype upstream from the gigantic exon. *Neurology* **66**, 1103–1104
6. Bouchard, R. W., Bouchard, J. P., Bouchard, R., and Barbeau, A. (1979) Electroencephalographic findings in Friedreich's ataxia and autosomal recessive spastic ataxia of Charlevoix-Saguenay (ARSACS). *Can. J. Neurol. Sci.* **6**, 191–194
7. Larivière, R., Gaudet, R., Gentil, B. J., Girard, M., Conte, T. C., Minotti, S., Leclerc-Desaulniers, K., Gehring, K., McKinney, R. A., Shoubridge, E. A., McPherson, P. S., Durham, H. D., and Brais, B. (2015) Sacs knockout mice present pathophysiological defects underlying autosomal recessive spastic ataxia of Charlevoix-Saguenay. *Hum. Mol. Genet.* **24**, 727–739
8. Duncan, E. J., Larivière, R., Bradshaw, T. Y., Longo, F., Sgarioto, N., Hayes, M. J., Romano, L. E. L., Nethisinghe, S., Giunti, P., Bruntraeger, M. B., Durham, H. D., Brais, B., Maltecca, F., Gentil, B. J., and Chapple, J. P. (2017) Altered organization of the intermediate filament cytoskeleton and relocalization of proteostasis modulators in cells lacking the ataxia protein sacsin. *Hum. Mol. Genet.* **26**, 3130–3143
9. Girard, M., Larivière, R., Parfitt, D. A., Deane, E. C., Gaudet, R., Nossova, N., Blondeau, F., Prenosil, G., Vermeulen, E. G., Duchen, M. R., Richter, A., Shoubridge, E. A., Gehring, K., McKinney, R. A., Brais, B., Chapple, J. P., and McPherson, P. S. (2012) Mitochondrial dysfunction and Purkinje cell loss in autosomal recessive spastic ataxia of Charlevoix-Saguenay (ARSACS). *Proc. Natl. Acad. Sci. USA* **109**, 1661–1666
10. Robert, A., Hookway, C., and Gelfand, V. I. (2016) Intermediate filament dynamics: what we can see now and why it matters. *BioEssays* **38**, 232–243
11. Herrmann, H., Häner, M., Brettel, M., Ku, N. O., and Aebi, U. (1999) Characterization of distinct early assembly units of different intermediate filament proteins. *J. Mol. Biol.* **286**, 1403–1420
12. Lee, M. K., Xu, Z., Wong, P. C., and Cleveland, D. W. (1993) Neurofilaments are obligate heteropolymers in vivo. *J. Cell Biol.* **122**, 1337–1350
13. Yuan, A., Rao, M. V., Veeranna, and Nixon, R. A. (2017) Neurofilaments and neurofilament proteins in health and disease. *Cold Spring Harb. Perspect. Biol.* **9**, a018309
14. Wiche, G., and Winter, L. (2011) Plectin isoforms as organizers of intermediate filament cytoarchitecture. *Bioarchitecture* **1**, 14–20
15. Cohlberg, J. A., Hajarian, H., and Sainte-Marie, S. (1987) Discrete soluble forms of middle and high molecular weight neurofilament proteins in dilute aqueous buffers. *J. Biol. Chem.* **262**, 17009–17015
16. Morris, J. R., and Lasek, R. J. (1982) Stable polymers of the axonal cytoskeleton: the axoplasmic ghost. *J. Cell Biol.* **92**, 192–198
17. Herrmann, H., and Aebi, U. (2004) Intermediate filaments: molecular structure, assembly mechanism, and integration into functionally distinct intracellular Scaffolds. *Annu. Rev. Biochem.* **73**, 749–789
18. Beaulieu, J. M., Nguyen, M. D., and Julien, J. P. (1999) Late onset of motor neurons in mice overexpressing wild-type peripherin. *J. Cell Biol.* **147**, 531–544
19. Côté, F., Collard, J. F., and Julien, J. P. (1993) Progressive neuronopathy in transgenic mice expressing the human neurofilament heavy gene: a mouse model of amyotrophic lateral sclerosis. *Cell* **73**, 35–46
20. Wong, N. K., He, B. P., and Strong, M. J. (2000) Characterization of neuronal intermediate filament protein expression in cervical spinal motor neurons in sporadic amyotrophic lateral sclerosis (ALS). *J. Neuropathol. Exp. Neurol.* **59**, 972–982
21. Wong, P. C., Marszalek, J., Crawford, T. O., Xu, Z., Hsieh, S. T., Griffin, J. W., and Cleveland, D. W. (1995) Increasing neurofilament subunit NF-M expression reduces axonal NF-H, inhibits radial growth, and results in neurofilamentous accumulation in motor neurons. *J. Cell Biol.* **130**, 1413–1422
22. Xu, Z., Cork, L. C., Griffin, J. W., and Cleveland, D. W. (1993) Increased expression of neurofilament subunit NF-L produces morphological alterations that resemble the pathology of human motor neuron disease. *Cell* **73**, 23–33
23. Ackerley, S., Thornhill, P., Grierson, A. J., Brownlees, J., Anderton, B. H., Leigh, P. N., Shaw, C. E., and Miller, C. C. (2003) Neurofilament heavy chain side arm phosphorylation regulates axonal transport of neurofilaments. *J. Cell Biol.* **161**, 489–495
24. Julien, J. P., and Mushynski, W. E. (1998) Neurofilaments in health and disease. *Prog. Nucleic Acid Res. Mol. Biol.* **61**, 1–23
25. Sánchez, I., Hassinger, L., Sihag, R. K., Cleveland, D. W., Mohan, P., and Nixon, R. A. (2000) Local control of neurofilament accumulation during radial growth of myelinating axons in vivo. Selective role of site-specific phosphorylation. *J. Cell Biol.* **151**, 1013–1024
26. Gentil, B. J., Minotti, S., Beange, M., Baloh, R. H., Julien, J. P., and Durham, H. D. (2012) Normal role of the low-molecular-weight neurofilament protein in mitochondrial dynamics and disruption in Charcot-Marie-Tooth disease. *FASEB J.* **26**, 1194–1203
27. Gentil, B. J., Mushynski, W. E., and Durham, H. D. (2013) Heterogeneity in the properties of NEFL mutants causing Charcot-Marie-Tooth disease results in differential effects on neurofilament assembly and susceptibility to intervention by the chaperone-inducer, celastrol. *Int. J. Biochem. Cell Biol.* **45**, 1499–1508
28. Nicholl, I. D., and Quinlan, R. A. (1994) Chaperone activity of alpha-crystallins modulates intermediate filament assembly. *EMBO J.* **13**, 945–953
29. Evgrafov, O. V., Mersiyanova, I., Irobi, J., Van Den Bosch, L., Dierick, I., Leung, C. L., Schagina, O., Verpoorten, N., Van Impe, K., Fedotov, V., Dadali, E., Auer-Grumbach, M., Windpassinger, C., Wagner, K., Mitrovic, Z., Hilton-Jones, D., Talbot, K., Martin, J. J., Vasserman, N., Tverskaya, S., Polyakov, A., Liem, R. K., Gettemans, J., Robberecht, W., De Jonghe, P., and Timmerman, V. (2004) Mutant small heat-shock protein 27 causes axonal Charcot-Marie-Tooth disease and distal hereditary motor neuropathy. *Nat. Genet.* **36**, 602–606
30. Irobi, J., Van Impe, K., Seeman, P., Jordanova, A., Dierick, I., Verpoorten, N., Michalik, A., De Vriendt, E., Jacobs, A., Van Gerwen, V., Vennekens, K., Mazanec, R., Tournev, I., Hilton-Jones, D., Talbot, K., Kremensky, I., Van Den Bosch, L., Robberecht, W., Van Vandekerckhove, J., Van Broeckhoven, C., Gettemans, J., De Jonghe, P., and Timmerman, V. (2004) Hot-spot residue in small heat-shock protein 22 causes distal motor neuropathy. *Nat. Genet.* **36**, 597–601
31. Tradewell, M. L., Durham, H. D., Mushynski, W. E., and Gentil, B. J. (2009) Mitochondrial and axonal abnormalities precede disruption of the neurofilament network in a model of Charcot-Marie-Tooth disease type 2E and are prevented by heat shock proteins in a mutant-specific fashion. *J. Neuropathol. Exp. Neurol.* **68**, 642–652
32. Anderson, J. F., Siller, E., and Barral, J. M. (2010) The sacsin repeating region (SRR): a novel Hsp90-related supra-domain associated with neurodegeneration. *J. Mol. Biol.* **400**, 665–674
33. Kozlov, G., Denisov, A. Y., Girard, M., Dicaire, M. J., Hamlin, J., McPherson, P. S., Brais, B., and Gehring, K. (2011) Structural basis of defects in the sacsin HEPN domain responsible for autosomal recessive spastic ataxia of Charlevoix-Saguenay (ARSACS). *J. Biol. Chem.* **286**, 20407–20412
34. Parfitt, D. A., Michael, G. J., Vermeulen, E. G., Prodromou, N. V., Webb, T. R., Gallo, J. M., Cheetham, M. E., Nicoll, W. S., Blatch, G. L., and Chapple, J. P. (2009) The ataxia protein sacsin is a functional co-chaperone that protects against polyglutamine-expanded ataxin-1. *Hum. Mol. Genet.* **18**, 1556–1565

35. Romano, A., Tessa, A., Barca, A., Fattori, F., de Leva, M. F., Terracciano, A., Storelli, C., Santorelli, F. M., and Verri, T. (2013) Comparative analysis and functional mapping of SACS mutations reveal novel insights into sacsin repeated architecture. *Hum. Mutat.* **34**, 525–537
36. Anantharaman, V., Makarova, K. S., Burroughs, A. M., Koonin, E. V., and Aravind, L. (2013) Comprehensive analysis of the HEPN superfamily: identification of novel roles in intra-genomic conflicts, defense, pathogenesis and RNA processing. *Biol. Direct* **8**, 15
37. Li, X., Ménade, M., Kozlov, G., Hu, Z., Dai, Z., McPherson, P. S., Brais, B., and Gehring, K. (2015) High-throughput screening for ligands of the HEPN domain of sacsin. *PLoS One* **10**, e0137298
38. Roy, J., Minotti, S., Dong, L., Figlewicz, D. A., and Durham, H. D. (1998) Glutamate potentiates the toxicity of mutant Cu/Zn-superoxide dismutase in motor neurons by postsynaptic calcium-dependent mechanisms. *J. Neurosci.* **18**, 9673–9684
39. Leung, C. L., and Liem, R. K. (2006) Isolation of intermediate filaments. *Curr. Protoc. Cell Biol.* Chapter 3, Unit 3.23
40. Heins, S., Wong, P. C., Müller, S., Goldie, K., Cleveland, D. W., and Aebi, U. (1993) The rod domain of NF-L determines neurofilament architecture, whereas the end domains specify filament assembly and network formation. *J. Cell Biol.* **123**, 1517–1533
41. Cohlberg, J. A., Hajarian, H., Tran, T., Alipourjeddi, P., and Noveen, A. (1995) Neurofilament protein heterotetramers as assembly intermediates. *J. Biol. Chem.* **270**, 9334–9339
42. Laser-Azogui, A., Kornreich, M., Malka-Gibor, E., and Beck, R. (2015) Neurofilament assembly and function during neuronal development. *Curr. Opin. Cell Biol.* **32**, 92–101
43. Boumil, E. F., Vohnoutka, R., Lee, S., Pant, H., and Shea, T. B. (2018) Assembly and turnover of neurofilaments in growing axonal neurites. *Biol. Open* **7**, 028795
44. Lee, S., Pant, H. C., and Shea, T. B. (2014) Divergent and convergent roles for kinases and phosphatases in neurofilament dynamics. *J. Cell Sci.* **127**, 4064–4077
45. Yoon, K. H., Yoon, M., Moir, R. D., Khuon, S., Flitney, F. W., and Goldman, R. D. (2001) Insights into the dynamic properties of keratin intermediate filaments in living epithelial cells. *J. Cell Biol.* **153**, 503–516
46. Hedberg, K. K., and Chen, L. B. (1986) Absence of intermediate filaments in a human adrenal cortex carcinoma-derived cell line. *Exp. Cell Res.* **163**, 509–517
47. Su, V., and Lau, A. F. (2009) Ubiquitin-like and ubiquitin-associated domain proteins: significance in proteasomal degradation. *Cell. Mol. Life Sci.* **66**, 2819–2833
48. Perng, M. D., Cairns, L., van den IJssel, P., Prescott, A., Hutcheson, A. M., and Quinlan, R. A. (1999) Intermediate filament interactions can be altered by HSP27 and alphaB-crystallin. *J. Cell Sci.* **112**, 2099–2112
49. Batulan, Z., Shinder, G. A., Minotti, S., He, B. P., Doroudchi, M. M., Nalbantoglu, J., Strong, M. J., and Durham, H. D. (2003) High threshold for induction of the stress response in motor neurons is associated with failure to activate HSF1. *J. Neurosci.* **23**, 5789–5798
50. Manzerra, P., and Brown, I. R. (1996) The neuronal stress response: nuclear translocation of heat shock proteins as an indicator of hyperthermic stress. *Exp. Cell Res.* **229**, 35–47
51. Deane, C. A., and Brown, I. R. (2016) Induction of heat shock proteins in differentiated human neuronal cells following co-application of celastrol and arimoclomol. *Cell Stress Chaperones* **21**, 837–848
52. Herrmann, H., Kreplak, L., and Aebi, U. (2004) Isolation, characterization, and in vitro assembly of intermediate filaments. *Methods Cell Biol.* **78**, 3–24
53. Benndorf, R., Martin, J. L., Kosakovsky Pond, S. L., and Wertheim, J. O. (2014) Neuropathy- and myopathy-associated mutations in human small heat shock proteins: characteristics and evolutionary history of the mutation sites. [E-pub ahead of print] *Mutat. Res. Rev. Mutat. Res.*S1383-5742(14)00018-0
54. He, Q., Liu, K., Tian, Z., and Du, S. J. (2015) The effects of Hsp90α1 mutations on myosin thick filament organization. *PLoS One* **10**, e0142573
55. Godsel, L. M., Hobbs, R. P., and Green, K. J. (2008) Intermediate filament assembly: dynamics to disease. *Trends Cell Biol.* **18**, 28–37
56. Laskey, R. A., Honda, B. M., Mills, A. D., and Finch, J. T. (1978) Nucleosomes are assembled by an acidic protein which binds histones and transfers them to DNA. *Nature* **275**, 416–420
57. Hirano, Y., Hendil, K. B., Yashiroda, H., Iemura, S., Nagane, R., Hioki, Y., Natsume, T., Tanaka, K., and Murata, S. (2005) A heterodimeric complex that promotes the assembly of mammalian 20S proteasomes. *Nature* **437**, 1381–1385
58. Ellis, R. J. (2013) Assembly chaperones: a perspective. *Philos. Trans. R. Soc. Lond. B Biol. Sci.* **368**, 20110398
59. Izawa, I., Nishizawa, M., Ohtakara, K., Ohtsuka, K., Inada, H., and Inagaki, M. (2000) Identification of Mrj, a DnaJ/Hsp40 family protein, as a keratin 8/18 filament regulatory protein. *J. Biol. Chem.* **275**, 34521–34527
60. Dekker, S. L., Kampinga, H. H., and Bergink, S. (2015) DNAJs: more than substrate delivery to HSPA. *Front. Mol. Biosci.* **2**, 35
61. Der Perng, M., Su, M., Wen, S. F., Li, R., Gibbon, T., Prescott, A. R., Brenner, M., and Quinlan, R. A. (2006) The Alexander disease-causing glial fibrillary acidic protein mutant, R416W, accumulates into Rosenthal fibers by a pathway that involves filament aggregation and the association of alpha B-crystallin and HSP27. *Am. J. Hum. Genet.* **79**, 197–213

Received for publication July 29, 2018.
Accepted for publication September 24, 2018.